

# The Effect of Varying Substituents on the Equilibrium Distribution and Conformation of Macrocyclic Steroidal *N*-Acyl Hydrazones

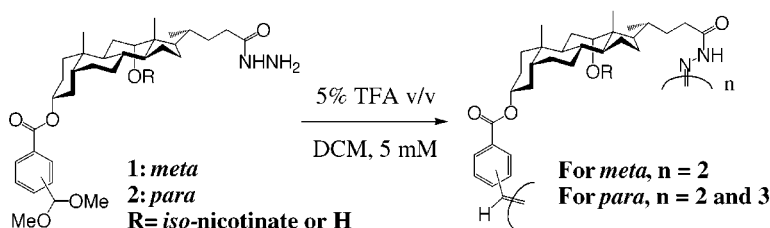
Mark G. Simpson, Stephen P. Watson,<sup>†</sup> Neil Feeder, John E. Davies, and Jeremy K. M. Sanders\*

University Chemical Laboratory, Lensfield Road, Cambridge, CB2 1EW, U.K.

jkms@cam.ac.uk

Received March 4, 2000

## ABSTRACT



The equilibrium distribution of deoxycholate-based macrocyclic *N*-acyl hydrazones is dependent upon the nature of the substituents at the 3- and 12-position. These substituents can also influence the preferred conformation of the macrocycles. The conversion of pure cyclic dimer and trimer into a mixture of both components, in the presence of trifluoroacetic acid, has been demonstrated and an X-ray crystal structure obtained of a macrocyclic *N*-acyl hydrazone dimer.

The tantalizing prospect of controlling interconverting libraries of molecular receptors, or guests, at equilibrium, by thermodynamic stabilization of selected species using a template, leading to in situ amplification, has captured the imagination of several groups.<sup>1</sup> The concept requires three features to succeed in principle: bond formation must be reversible; several products should be formed at equilibrium, upon which the selection process can act; and the molecules themselves must possess recognition potential.

Attention within this group focused initially upon transesterification in order to demonstrate thermodynamic templating on a mixture of receptors at equilibrium. To employ organic templates, however, our efforts have shifted to the

consideration of transimination as a means of satisfying the requirement for reversibility.

Interconversion of imine-based macrocycles has been reported to proceed under acid catalysis at ambient temperatures and to be under thermodynamic control.<sup>2</sup> The closely related *N*-acyl hydrazones have been largely overlooked, as far as the construction of supramolecular architectures and development of reversible chemistry are concerned.<sup>3</sup> They possess, however, several attractive features: formation is reversible, yet goes to completion; they are easily accessible and robust and contain hydrogen bond donor and acceptors in the amide group (Scheme 1) enabling potential peptide-type recognition.

Many elegant examples of steroid-based macrocyclic receptors have been synthesized, under kinetic control, by Davis<sup>4</sup> and Bonar-Law<sup>5</sup> and thermodynamic control by Brady

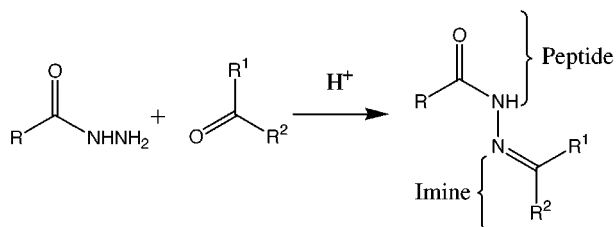
<sup>†</sup> GlaxoWellcome, Medicines Research Centre, Stevenage, Herts, SG1 2NY.

(1) (a) Still, W. C.; Hauck, P.; Kempf, D. *Tetrahedron Lett.* **1987**, 28, 2817–2820. (b) Hioki, H.; Still, W. C. *J. Org. Chem.* **1998**, 63, 904–905. (c) Lehn, J.-M. *Chem. Eur. J.* **1999**, 5, 2455–2463. (d) Brady, P. A.; Sanders, J. K. M. *J. Chem. Soc., Perkin Trans. 1* **1997**, 3237–3253. (e) Calama, M. C.; Timmerman, P.; Reinhoudt, D. N. *Angew. Chem., Int. Ed.* **2000**, 39, 755–758.

(2) Hockless, D. C. R.; Lindoy, L. F.; Swiegers, G. F.; Wild, S. B. *J. Chem. Soc., Perkin Trans. 1* **1998**, 117–122.

(3) Cousins, G. R. L.; Poulsen, S.-A.; Sanders, J. K. M. *J. Chem. Soc., Chem. Commun.* **1999**, 16, 1575–1576.

**Scheme 1.** Reaction of an Acyl Hydrazide with a Carbonyl Compound To Form an Acyl Hydrazone



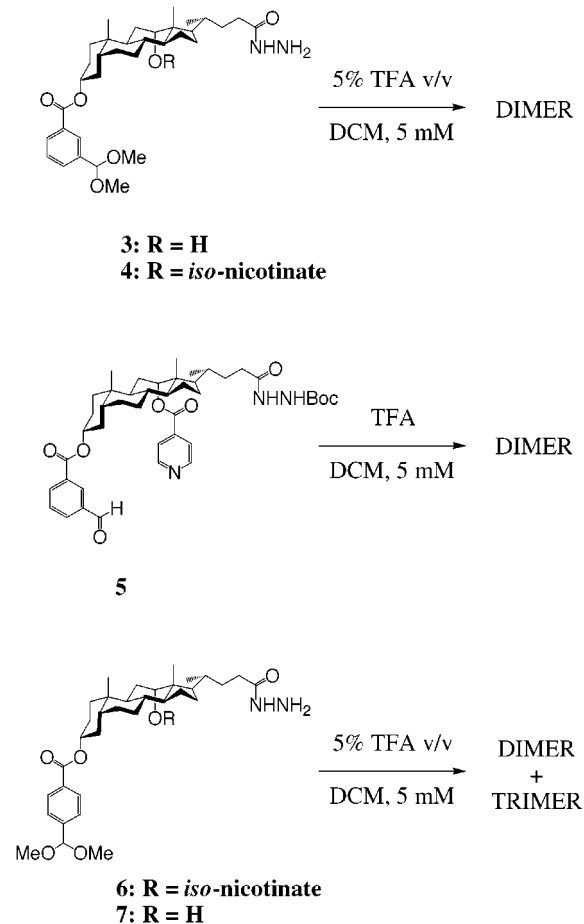
et al.<sup>6</sup> Deoxycholic acid thus seemed a promising choice for the construction of potential *N*-acyl hydrazone-based receptors.

The reaction between hydrazine and the carbonyl group is rapid and quantitative at ambient temperatures (Scheme 1) so in order to control macrocyclization it is necessary to protect either the hydrazine or carbonyl functionality. Protection of the carbonyl component as its dimethyl acetal and installation of the hydrazide via hydrazinolysis<sup>7</sup> or the use of the Boc-protected hydrazide<sup>8</sup> followed by deprotection gave rise to the same product distribution, though the former proved to be more synthetically convenient.

Herein we report a series of protected steroid-based hydrazides and the nature of the cyclic hydrazones formed upon deprotection. With the *meta*-substituted aldehydes **3–5** (Scheme 2), deprotection, using trifluoroacetic acid, led to the formation of a single product, the cyclic dimer. When the geometry of the aldehyde was changed to *para*, however, in the case of **6** and **7** (Scheme 2), two cyclic products, the dimer and trimer, were observed. In the case of the *meta*-substituted aldehyde, varying the substituent at the 12-position, from *iso*-nicotinate to hydroxyl, did not lead to any change in the distribution of products. This did, however, lead to a change in the shape of the dimer. For the *para*-substituted steroid, changing the substituent from *iso*-nicotinate to hydroxyl led to a significant decrease in the amount of cyclic trimer formed at equilibrium, under comparable conditions. In all cases 1- and 2-D NMR indicated the presence of a single conformation of the cyclic hydrazone, where several are clearly possible.<sup>9</sup>

The deoxycholate-based protected hydrazide monomers (**3–7**) (Scheme 2) were synthesized from deoxycholic acid in respectable overall yields (40–60%) and gave satisfactory <sup>1</sup>H and <sup>13</sup>C NMR spectra, microanalysis, IR, and ESI-MS. Deprotection of a 5 mM solution of the deoxycholate acetal hydrazides (**3**, **4**, **6**, and **7**) in freshly distilled, dry DCM or CHCl<sub>3</sub> was achieved by adding trifluoroacetic acid (TFA)

**Scheme 2.** Effect of Geometry on the Distribution of Cyclic Products Formed after Deprotection



(5% v/v). Deprotection of **5** was accomplished using neat TFA, followed by dilution with DCM. These procedures led to rapid, clean formation of the cyclic hydrazones in a matter of minutes with no linear, uncyclized species detectable by HPLC or ESI-MS. The initial distribution did not change over a period of days, and following neutralization of the reaction mixture with triethylamine, the pure macrocycles were isolated by preparative TLC.

**3** gave rise to a single product, the cyclic dimer **8** (Figure 1), according to ESI-MS, in quantitative yield. Both COSY and NOESY experiments upon **8** in CDCl<sub>3</sub> support the assignments shown. The broad hydrazone NH singlet at 9.34 ppm exhibits a strong NOE cross-peak to the azamethine proton, H<sub>μ</sub>, at 7.55 ppm, confirming the *cis*, *E* arrangement shown. Since there is no NOE cross-peak from the hydrazone NH to the 22- or 23-protons at 2.57 and 2.96 ppm, it seems unlikely that it is directed into the cavity. A strong NOE cross-peak can be identified between the azamethine proton, H<sub>μ</sub>, at 7.55 ppm and H<sub>γ</sub> at 8.08 ppm. A weak NOE cross-peak between the azamethine proton, H<sub>μ</sub>, at 7.55 ppm and H<sub>γ</sub> at 8.51 ppm implies that the hydrazone geometry may be twisted somewhat.

**4** and **5** both gave rise to cyclic dimer **9** (Figure 1) according to ESI-MS, isolable in 90% yield. COSY and NOESY spectra of **9** in CDCl<sub>3</sub> revealed a quite different

(4) Davis, A. P. *Chem. Soc. Rev.* **1993**, 22, 243–253.  
(5) Bonar-Law, R. P.; Sanders, J. K. M. *J. Am. Chem. Soc.* **1995**, 117, 259–271.  
(6) Brady, P. A.; Bonar-Law, R. P.; Rowan, S. J.; Suckling, C. J.; Sanders, J. K. M. *J. Chem. Soc., Chem. Commun.* **1996**, 319–320.  
(7) Lenman, M. M.; Lewis, A.; Gani, D. *J. Chem. Soc., Perkin Trans. 1* **1997**, 2297–2311.  
(8) Gordon, M. S.; Krause, J. G.; Linneman-Mohr, M. A.; Parchue, R. *Synthesis* **1980**, 244–245.  
(9) Palla, G.; Predieri, G.; Domiano, P.; Vignali, C.; Turner, W. *Tetrahedron* **1986**, 42, 3649–3654.

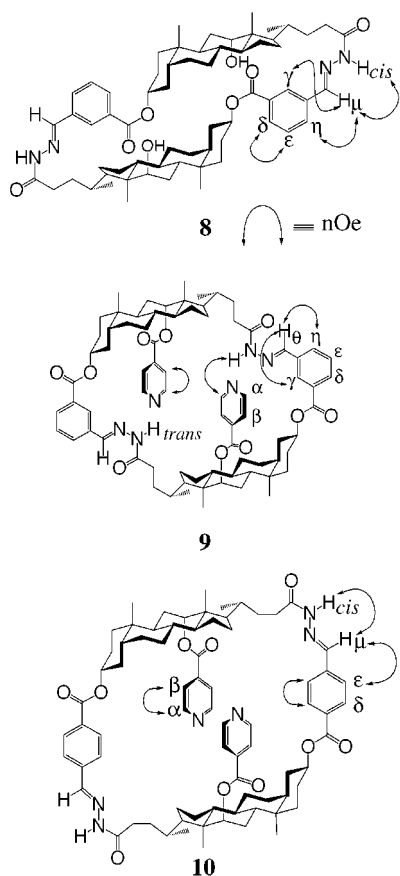


**Figure 1.** Selected NOEs for a series of macrocyclic hydrazones to illustrate the differing geometries.

structure compared to that of **8**. The lack of an NOE connectivity between the hydrazone NH at 10.85 ppm and the azamethine proton,  $H_\theta$ , at 8.62 ppm, suggests a *trans*, *E* arrangement of the hydrazone. The conclusion that the hydrazone NH is directed into the cavity also appears to be supported by the presence of a weak NOE cross-peak between itself at 10.85 ppm and the  $\alpha$ -pyridyl proton of the *iso*-nicotinate substituent at 8.65 ppm. The azamethine proton,  $H_\theta$ , at 8.62 ppm has weak NOEs to  $H_\eta$  at 7.87 ppm and  $H_\gamma$  at 7.85 ppm, supporting, once again, a twisted hydrazone geometry. There are also weak NOEs between the hydrazone NH and the two 23-protons. The construction of CPK models suggests that it might be possible for two *intramolecular* hydrogen bonds to be formed in the cyclic dimer, thus explaining why this conformation is favored.

By way of contrast, deprotection of a 5 mM solution of **6**, in DCM with 5% trifluoroacetic acid v/v, led to the formation of two cyclic products, as evidenced by HPLC, ESI-MS, and  $^1\text{H}$  NMR spectroscopy. ESI-MS revealed peaks at 626,  $[\text{M} + 2\text{H}]^{2+}$ , 939  $[\text{M} + 2\text{H}]^{2+}$ , 1251  $[\text{M} + \text{H}]^+$ , and 1877  $[\text{M} + \text{H}]^+$ , consistent with the formation of cyclic dimer **10** (Figure 1) and trimer **11** (Figure 2). HPLC indicated the formation of dimer:trimer in a 3:1 ratio. These two cyclic products could be separated by preparative TLC to afford the dimer **10** and trimer **11** as pure, stable materials and hence to confirm the HPLC and ESI-MS assignments individually.

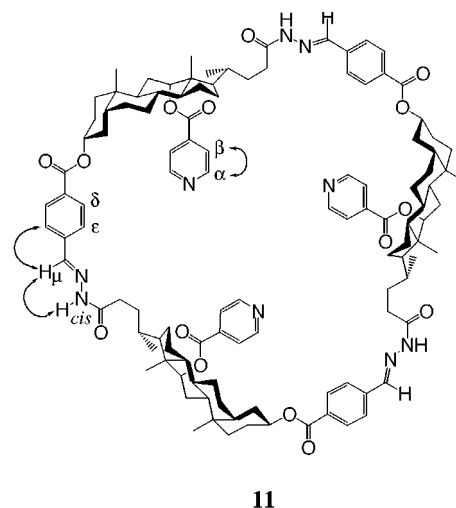


**Figure 2.** Selected NOEs for the steroidal hydrazone trimer **11**.

A NOESY experiment on **10** in  $\text{CDCl}_3$  revealed the geometry of the hydrazone linkage as *cis*, *E*. An NOE connectivity was observed between the azamethine proton,  $H_\mu$ , at 7.64 ppm and the hydrazone NH at 9.17 ppm but not between the hydrazone NH and the 23-H steroid protons. A further NOE connectivity was observed between the azamethine proton and  $H_\epsilon$  (Figure 1). The NOESY spectrum of the cyclic trimer **11** also indicated a *cis*, *E* hydrazone geometry (Figure 2).

It proved possible to grow crystals of **10** suitable for the determination of the X-ray crystal structure by slow evaporation of a solution of **10** in  $\text{CD}_2\text{Cl}_2$ . This also revealed a *cis*, *E* hydrazone geometry, together with a planar acyl hydrazone unit and conjugation of the imine with the aromatic ring (Figure 3).

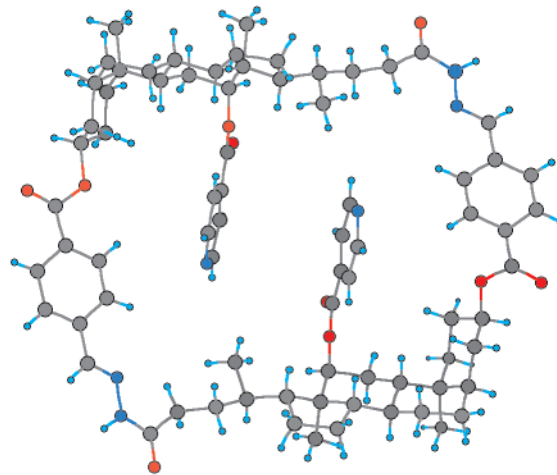


**Figure 3.** Ball and stick representation of the X-ray crystal structure of the cyclic hydrazone dimer **10**. Disorder around *iso*-nicotinate not shown.

By HPLC and ESI-MS it was possible to show that a 2.5 mM solution of pure **10** in DCM could be converted into a mixture of **10** and **11** by adding 2.5% trifluoroacetic acid v/v and vice versa with an appropriate concentration of pure trimer. Equilibrium was typically attained after 6 h. This, together with the dependence of the ratio of dimer **10** and trimer **11** on the initial concentration of **6**, demonstrates that macrocyclic steroid-based hydrazone formation is both reversible and under thermodynamic control (Figure 4).<sup>10</sup>

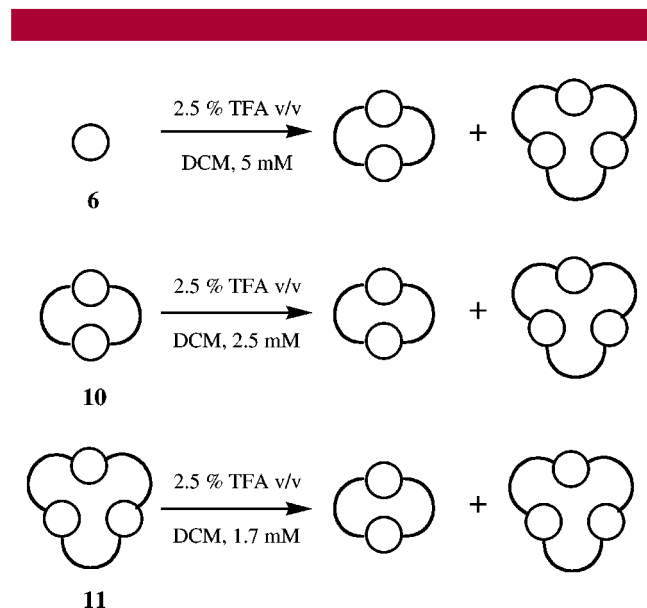


**Figure 4.** Illustrating the reversibility of steroid-based macrocyclic hydrazone formation. In all cases the ratio of **10**:**11** was 3:1 at equilibrium.

In comparison, deprotection of identical concentrations of **7** led to much less cyclic trimer at equilibrium. Deprotection of **7** at a concentration of 5 mM in DCM led to a dimer:trimer ratio of 8:1 while increasing the concentration of **7** to 10 mM changed the distribution to 6:1, as judged by HPLC. This is interesting and clearly suggests that the *iso*-nicotinate group has some role to play in either stabilizing the formation of trimer **11** or perhaps destabilizing dimer **10**.

This work demonstrates that the nature of the substituents at the 3- and 12-position are intimately involved in controlling the equilibrium distribution of macrocyclic steroidal hydrazones. In addition, the reversibility of *N*-acyl hydrazone formation, involving steroid-based hydrazones, has also been demonstrated. This process has been shown to be catalyzed by trifluoroacetic acid and to be under thermodynamic control.<sup>11</sup>

**Acknowledgment.** We thank both BBSRC and Glaxo-Wellcome for financial support (M.G.S.) and Dr. Nick Bampos for running 500 MHz COSY and NOESY NMR spectra.

**Supporting Information Available:** Microanalysis, IR, ESI-MS, and <sup>1</sup>H and <sup>13</sup>C NMR spectral data for monomers **3**, **4**, **5**, **6**, and **7**. IR, ESI-MS, and <sup>1</sup>H and <sup>13</sup>C NMR spectral data for macrocycles **8**, **9**, **10**, and **11**. Crystallographic data for macrocyclic hydrazone **10**. This material is available free of charge via the Internet at <http://pubs.acs.org>.

OL005754X

(10) Ercolani, G.; Mandolini, L.; Mencarelli, P.; Roelens, S. *J. Am. Chem. Soc.* **1993**, *115*, 3901–3908.

(11) The behavior of steroid-based hydrazides contrasts markedly with amino acid-based hydrazides. In the case of amino acid-based monomers, a wide range of macrocycles were formed at equilibrium according to ESI-MS. See ref 3 for more details.